Int. J. Electrochem. Sci., 14 **(2019)** 1372 – 1387, doi: 10.20964/2019.02.29

International Journal of
ELECTROCHEMICAL
SCIENCE
www.electrochemsci.org

Corrosion Control of Copper in Nitric Acid Solution using Chenopodium Extract

M. M. Motawea[1], *A.El-Hossiany*[2], *A. S. Fouda*[3,*]

[1] Department of Chemistry, College of Science, University of Bisha, Bisha, Kingdom of Saudi Arabia and Misr Higher Institute of Engineering & Technology Mansoura, Egypt
[2] Chemist, Delta Fertilizers Company in Talkha, Egypt.
[3] Chemistry Department, Faculty of Science, Mansoura University, Mansoura-35516, Egypt,
[*]E-mail: asfouda@hotmail.com

Received: 9 October 2018 / *Accepted:* 6 December 2018 / *Published:* 5 January 2019

Chenopodium extract was examined as a corrosion inhibitor for Cu in 1M HNO_3 by utilizing chemical and electrochemical techniques. The results displayed that Chenopodium extract (CE) could play important role as a corrosion inhibitor for Cu in 1 M HMO_3. The protection efficiency (PE) increases with rise of the CE concentrations (reached to > 92%) due to the adsorption of the CE molecules on the Cu surface. Furthermore, it was recognized that the adsorption obeyed Langmuir isotherm. The polarization data showed that this CE acts as mixed kind inhibitor. In addition some thermodynamic data were measured and explained.

Keywords: Corrosion inhibition, Cu, HNO_3, Chenopodium extract, Adsorption

1. INTRODUCTION

Cu is a metal that has a varied range of applications because it’s excellent thermal conductivity and mechanical properties. It is utilized in electronics, for manufacture of wires, tubes, sheets, and also to form metal alloys. Cu is a comparatively noble metal. However, it reacts easily in ordinary, oxygen inclosing, environments. The probability of the Cu corrosion protection in various aqueous solutions has attracted many researchers so until now several possible inhibitors have been examined. Corrosion protection can be distinct as substances that are present in little quantities to the environment in order to decrease further dissolution of the metal. While the inhibitor selecting depends on various factors, for example, its toxicity, cost, accessibility and environment friendliness necessity to be considered. During the recent two decades a lot of consideration has been paid to area of "green inhibitors". A large portion of the examinations were directed near search for cheap, effective molecules with little or ‘‘zero’’ impact on environment and human health [1– 4]. Many authors reported the use of plant extracts as save corrosion inhibitors for various metals and alloys under different environments, such as: Citrus aurantium for Cu in HNO_3 [5], Ceratonia siliqua for Cu in HNO_3[6], Ailanthus Altissima for Zn in HCl [7], Artemisia Judaica Herbs for carbon steel in HCl [8], Cassia italic for carbon steel in H_2SO_4 [9], Ferula Hermonis for SS430 in HCl [10], Berry Leaves for Cu in HNO_3 [11], tetraclinis articulate for mild steel in HCl [12], Punica Granatum for Al in HCl [13], Cleome Droserifolia (Samwah) for mild steel in HCl [14], Cassia Angustifolia (Senna) Fruit for mild steel in HCl [15] and Rumex Vesicarius L for carbon steel in H_2SO_4 [16]. The use of CE as corrosion inhibitor is due to: it is biodegradable, do not contain heavy metals or toxic compounds, inexpensive, readily available, renewable as well as environmentally friendly.

The current study aims to evaluate the corrosion inhibition properties of CE as eco-friendly corrosion inhibitor on the electrochemical behavior of Cu in aqueous nitric acid at different temperatures.

2. EXPERIMENTAL METHOD

2.1 Materials and Solutions

Table 1. Describes chemical conformation of the Cu in percentage weight

Element	Sn	Fe	Ag	Bi	Pb	As	Cu
Wt %	0.001	0.01	0.001	0.005	0.002	0.0002	The rest

The experimental methods were done in 1 M HNO_3 solution with and without various concentrations of Chenopodium extract

2.2 Plant Extract Preparation Method:

Chenopodium ambrosioides L., popularly known as Santa Maria herb and Paico, is a medicinal plant which, for centuries, has been popularly used for its medicinal properties [17]. The wide use of the Santa Maria herb is due to the presence of high levels of ascaridole in the seeds, leaves, and stem. It is mainly used for the treatment of ascaridiasis, and has been demonstrated to be effective in the control of *Ascaridia* sp. in Japanese quails [18]. Few authors have reported the efficacy of the aqueous extract against gastrointestinal nematodes in small ruminants [19] and hexane and dichloromethane extracts against *Toxocara canis* larvae [20]. A Plant utilized in this assignment collected from the Sadat city desert, Egypt. Chenopodium were pre washed and then dried in air at room temperature away from direct light. The extract was obtained by soaking 200 g of the Chenopodium powder with 70% methanol for 48 hr. The powder was removed by filtration to get clear filtrate consequently, the filtrate was vaporized under vacuum, and the remainder was collected and stored in refrigeration in glass flasks peaked with screw plastic lid. It was confirmed that extract consists protocatechuic acid, p- hydroxyl benzoic acid , Gallic acid, vallinic acid, thymine, caffeic acid, 5,7-dihydroxy chromone, and luteolin.

2.3 Technique Utilized for Corrosion Tests

2.3.1 Mass Loss (ML) Tests:

The square coins with size (2 cm x 2cm x 0.2cm) were soaking in 100 ml of 1M HNO_3 with and without various concentrations of Chenopodium are set in water thermostat. After 3 h the samples were removed, rinsed, dried, and weighed again [21]. The % PE and the θ were established from Eq. (1)

$$\% \text{ PE} = \theta \times 100 = [1-(W/W^o)] \times 100 \qquad (1)$$

Where W^o and W are the weights in absence and presence of Chenopodium, respectively.

2.3.2 Potentiodynamic Polarization (PP) Tests:

PP method was taken in a typical three compartments glass cell. The potential range was (-800 to +200 mV vs. SCE) at OCP with a scan rate 1 mVs^{-1}.

Then i_{corr} was calculated for the measurements and was used to calculate the PE and the θ from Eq. (2) as below:

$$\%\text{PE} = \theta \times 100 = [1-(i_{corr}/i^o_{corr})] \times 100 \qquad (2)$$

2.3.3 Electrochemical Impedance Spectroscopy (EIS) Tests:

EIS measurements were done by AC signs of 5 mV peak-to-peak amplitude and at range of frequency of 10^7 Hz to 0.1Hz.

2.3.4 Electrochemical Frequency Modulation (EFM) Tests:

This method utilized two frequencies of variety 2 Hz and 5 Hz rely on three conditions [22-24]. The (i_{corr}), (β_c and β_a) and (CF-2, CF-3) (Causality factors) were measure by the greater two peaks [25].

2.4 Surface Examinations:

The Cu samples were dipped in 1 M HNO_3 without and with the CE at 25°C for 1day. The examination was accepted by utilizing SEM (JEOL JSM-5500, Japan). Pico SPM 2100 AFM device also utilized to examine the shape of Cu surface. IR Affinity (Perkin-Elmer) spectrophotometer was utilized for estimate the FTIR spectra to measure the composition of the corrosion creation designed on the Cu surface.

3. RESULTS AND DISSCUSSION

3.1 Chemical Method (ML tests)

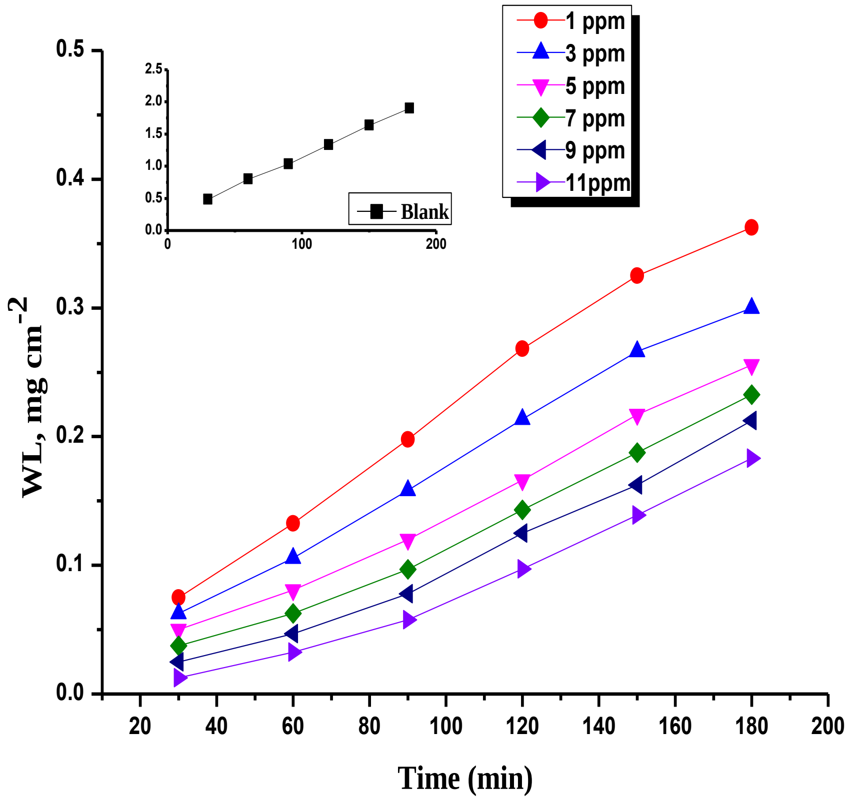

Figure 1. ML-time diagrams for the Cu in 1 M HNO_3 without and with various concentrations of CE at 25^{o}C

The mass loss of Cu can be studied in presence of CE at 25°C. Figure 1 shows that CE lowers the ML and therefore the corrosion rate. The (% PE) and then θ, of the CE for the Cu were estimated from eq. (1). The values of % PE are given in Table 2.

Table 2. Values of % PE and θ after 120 min of Cu in 1 M HNO_3 without and with various concentrations of Chenopodium at 25°C

[inh] , ppm	θ	% PE
1	0.785	78.5
3	0.831	831
5	0.878	87.8
7	0.897	89.7
9	0.906	90.6
11	0.915	91.5

3.2 Influence of Temperature

The effect of temperature on the rate of corrosion of Cu in 1 M HNO_3 with and without various CE concentrations was examined in the range of temperature range 298–313K utilizing ML tests. The results of Table 3 indicate that the rise in % PE with the increase in the temperature proved the presence of chemical adsorption of CE on Cu surface.

Table 3. Parameters (% PE and (C.R.)) for Cu dissolution after 120 min without and with various concentrations of CE at different temperatures

[Inh], ppm	298		303K		308K		313K		318K	
	C.R	% PE	C.R	%PE	C.R	%PE	C.R	%PE	C.R	%PE
1	2.39	78.5	4.27	81.1	5.20	83.7	5.93	86.1	7.29	86.3
3	1.87	83.1	2.91	87.0	4.06	87.3	5.10	88.1	5.93	88.8
5	1.35	87.8	2.5	88.9	3.33	89.6	4.16	90.2	4.79	91.0
7	1.14	89.7	2.08	90.7	2.91	90.9	3.85	91.0	4.27	92.0
9	1.04	90.6	1.97	91.2	2.60	91.8	3.43	91.9	4.06	92.3
11	0.937	91.5	1.77	92.1	2.29	92.8	2.81	93.4	3.22	93.9

3.3. Kinetic –Thermodynamic Corrosion

Arrhenius equation (3) can be utilized to measure the (E^*_a) of the activated energy according to eq. (3):

$$k_{corr} = A \exp (E^*_a/RT) \qquad (3)$$

Where E^*_a is activation energy and T is the absolute temperature. Using Figure 2, E^*_a can be measured (Table 4). E^*_a values prove that the higher percentage of CE impede corrosion effectively by raising the energy barrier of the activated complex and improve that the process is controlled by diffusion [26, 27]. The decrease of E^*_a by rising the concentrations of CE, indicates that CE was adsorbed chemically on Cu surface [28]

(ΔH^*, ΔS^*) are measured by eq. (4) [29]:

$$k_{corr.} = RT / Nh \exp (\Delta S^*/R) \exp (-\Delta H^*/ RT) \qquad (4)$$

Figure 3 shows the relation between log (k_{corr} /T) and (1/T) which used to measure the values of ΔH^* and ΔS^*(Table 4). The raising in E_a^* with rise CE dose Table 4 is typical of physical adsorption. The positive signs of ΔH^* reflect the endothermic nature of the Cu dissolution process. The negative values of ΔS^* shows that during the rate-determining step, the formation of activated complex is more ordered than that the reactants [30]

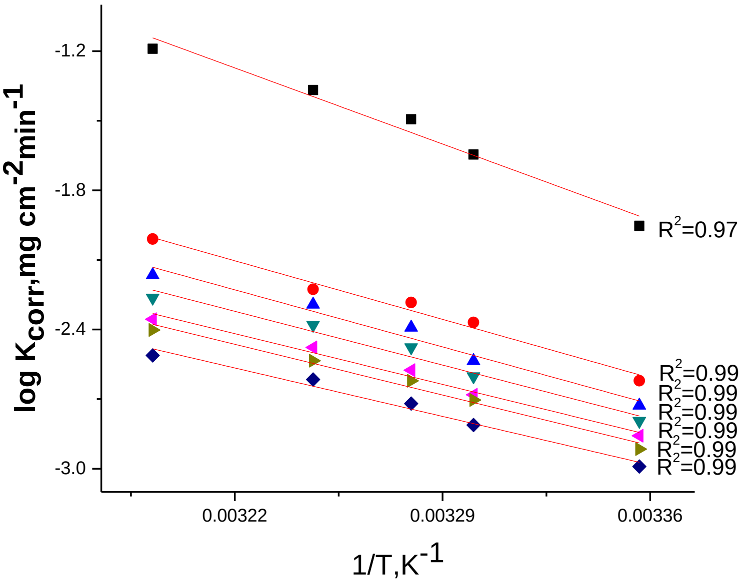

Figure 2. Arrhenius curves for Cu dissolution after 120 min immersion in 1 M HNO_3 without and with various CE concentrations

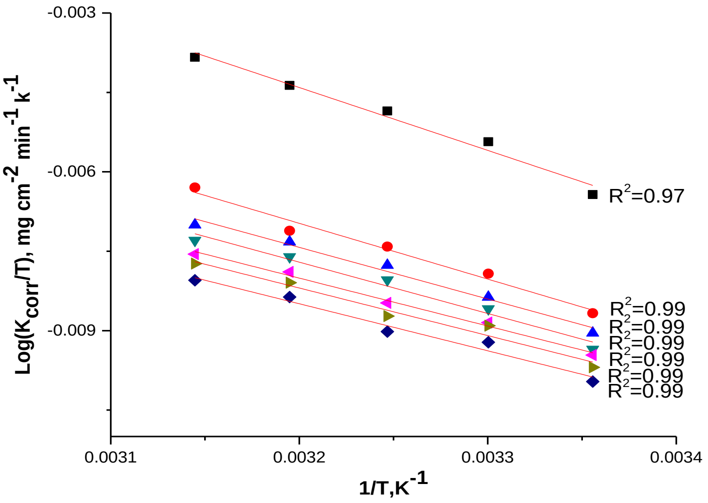

Figure 3. Plots log (k_{corr}/T) and 1/T diagrams for the Cu without and with different CE concentrations

Table 4. Activation parameters for Cu without and with various concentrations of CE in 1 M HNO_3

[Inh], ppm	E_a^*, kJ mol^{-1}	ΔH^* kJ mol^{-1}	-ΔS^* J mol^{-1}
0	89.7	220.8	196.8
1	69.0	196.8	196.9
3	67.3	181.0	197.05
5	63.4	180.0	197.06
7	59.8	169.0	197.1
9	59.7	168.0	197.10
11	57.1	166.0	197.11

3.4 Adsorption Isotherms

Figure 4 represents the Langmuir isotherm, which utilized to measure ϴ values for additives CE. The Langmuir relation represented as next.

$C/\Theta=1/K_{ads}+C$ (5)

Where K_{ads} is the adsorption constant and Cis the CE content (M)

The $\Delta G°_{ads}$ and K_{ads} data are represented in Table 5, 6. The ΔG^{o}_{ads} established by**:**

$\Delta G^{o}_{ads} = - RT \ln (55.5\ K_{ads})$ (6)

The CE adsorption is spontaneous and this is proved by the negative sign of $\Delta G°_{ads}$. From the data of ΔG^{o}_{ads} (more than-20 kJ mol^{-1}), proven that the CE adsorption is mixed one (physisorption and chemisorption) [31].

Vant't Hoff equation can be utilized to measure $\Delta H°_{ads}$ and $\Delta S°_{ads}$ [16] expressed by eq. (7):

$\Delta G^{o}_{ads} = \Delta H^{o}_{ads} - T\ \Delta S^{o}_{ads}$ (7)

Figure 5 shows the relation among ΔG^{o}_{ads} and T. A positive sign of ΔS^{o}_{ads} proved that the disorder of corrosion procedure is rise by utilizing Chenopodium (Table 6).

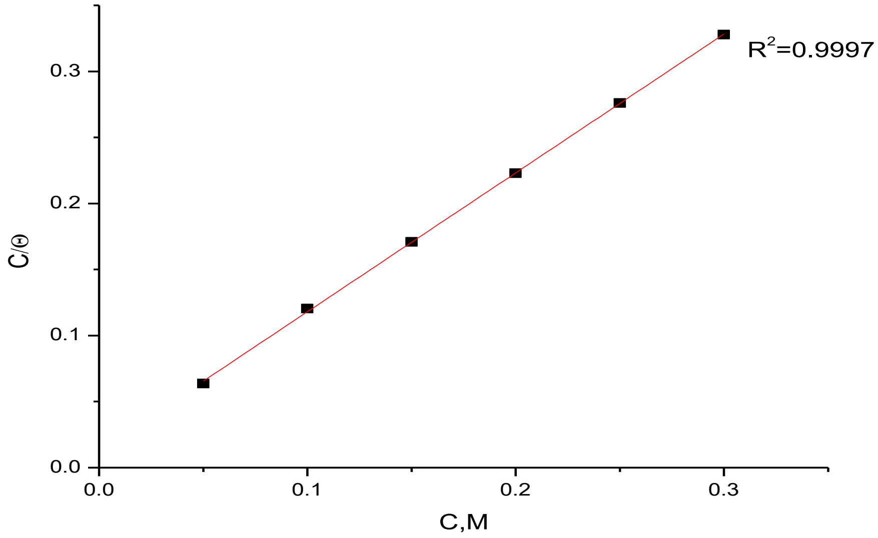

Figure 4. Langmuir isotherm for the CE on Cu in 1M HNO_3 at 298K

Table 5. Parameters for CE in 1 M HNO_3 obtained from Langmuir isotherm at various temperatures

Temp., °C	K_{ads}, M^{-1}
25	77.2
30	107.4
35	117.4
40	136.0
45	142.5

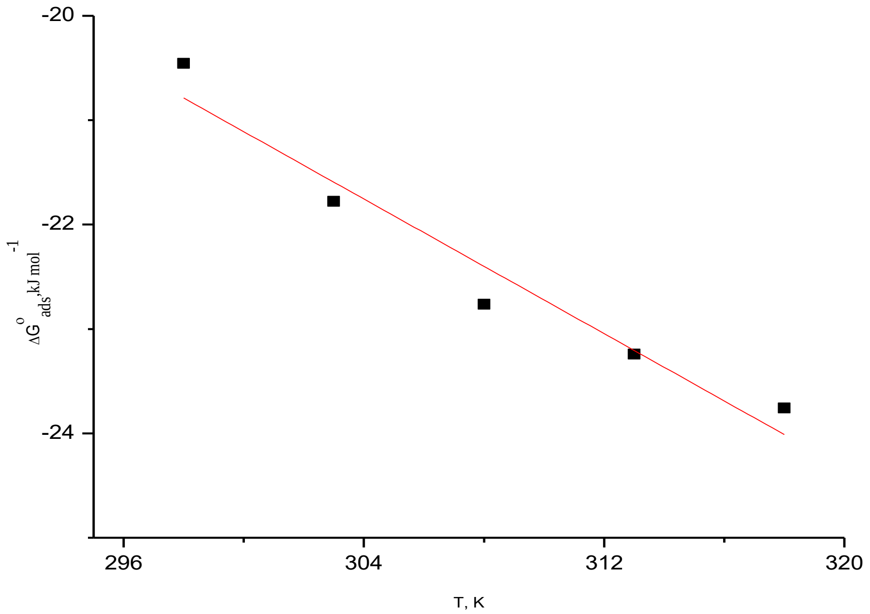

Figure 5. Plots of ΔG^o_{ads} against T for the adsorption of CE on Cu surface in 1 M HNO_3 at various temperatures

Table 6. Langmuir data for Cu in 1 M HNO_3 without and with using various CE concentrations at (25°C-45°C)

Temp., °C	$-\Delta G^o_{ads}$ kJ mol^{-1}	ΔH^o_{ads} kJ mol^{-1}	ΔS^o_{ads} J mol^{-1}K^{-1}
25	20.7	27.3	162.0
30	21.9		160.9
35	22.5		160.5
40	23.2		160.3
45	23.7		159.8

3.5 Potentiodynamic Polarization (PP) Tests

Tafel diagrams of Cu electrode in 1M HNO_3 with and without various concentrations of CE can be studied from Figure 6. From Table 7 CE has effect on both of cathodic, anodic processes and the PE rises with rise of the CE concentrations. E_{corr} was a little changed, indicating that CE acts as a mixed type inhibitor. i_{corr} reduced among the CE addition to 1M HNO_3.

Various corrosion parameters for example: [($E_{corr.}$), (β_a, β_c), (i_{corr}), (θ) and (%IE)] are reported in Table 7.

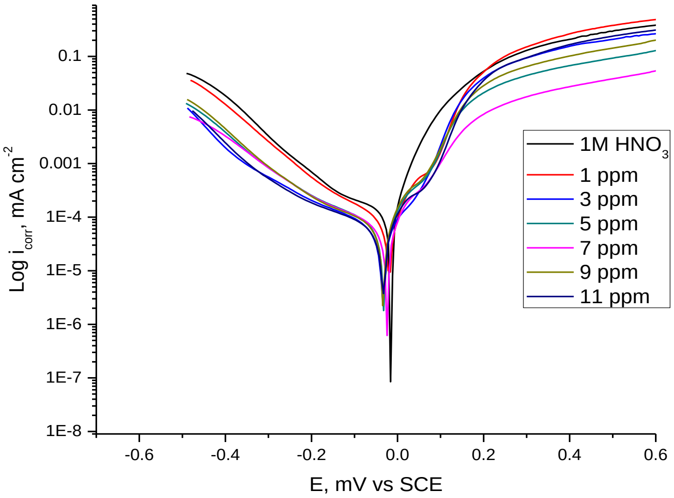

Figure 6. Potentiodynamic Polarization diagrams of the Cu dissolution with and without various concentrations of CE at 25^{o}C

Table 7. Potentiodynamic Polarization results of Cu dissolution with and without various concentrations of CE at 25^{o}C

[inh], ppm	-E$_{corr}$ mV vs SCE	i$_{corr}$x10^{-4} µA cm^{-2}	β$_a$, mV dec^{-1}	β$_c$, mV dec^{-1}	k$_{corr}$ mpy	ϴ	% PE
0	16.2	512	110	222	252	--	--
1	19.1	103	82	283	47	0.80	80
3	32.9	79.8	88	252	37	0.844	84.4
5	24.6	79	95	277	36	0.846	84.6
7	33.6	74.1	87	238	34	0.855	85.5
9	33.9	73.7	97	227	33	0.856	85.6
11	33.9	68.9	89	292	31	0.865	86.5

3.6 Electrochemical Impedance Spectroscopy (EIS) Tests

EIS tests were utilized to study the mechanism of corrosion. The results of Nyquist and Bode diagrams are demonstrated in Figure 8a, 8b, respectively, and these figures displayed a gradual increamet in the semicircle diameter of the Nyquist diagrams by raising the dose of CE. So the CE molecules retard the corrosion rate [32-38]. From Figure 8a we noticed that the deviation from an ideal semicircle as a result of frequency dispersion because the inhomogeneity of the surface [39-42]. Table 8 gives different parameters of impedance as, resistance charge transfer (R_{ct}), double layer capacitance (C_{dl}), protection efficiency (PE) and electrolyte resistance (R_s). The data of Table 8 demonstrated that, the C_{dl} data lowered by raising the dose of CE, this behavior as a result of molecules adsorbed on the surface of Cu, and this demonstrated from Helmholtz model, where the capacitance of double layer was obtain by the next relation [43]. Figure 7 reveals to equivalent circuit which used in our study [44].

The data of double layer capacity were measured from the next relation [45]:

$C_{dl} = Y_0\ (\omega_{max})^{\ n-1}$ (9)

whereY_0 is the magnitude of the CPE, $\omega_{max} = 2\pi f_{max}$, f_{max} is the frequency at which the imaginary component of the impedance is maximal and the factor n is an adjustable parameter that typically lies among 0.50 and 1.0.

The data of PE which found in Table 8 were measured from the next relation:

$\%\ PE= 100X\theta = [1-(R^0_{ct}/R_{ct})]$ (10)

Where R^0_{ct} and $R_{ct}$are the charge transfer resistances with and without addition of different concentrations of CE, respectively

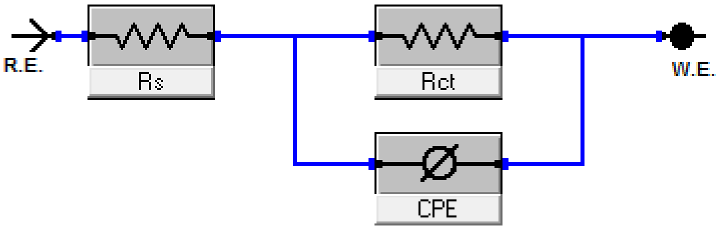

Figure 7. Circuit utilized for fitting the data of EIS in 1 M HNO_3

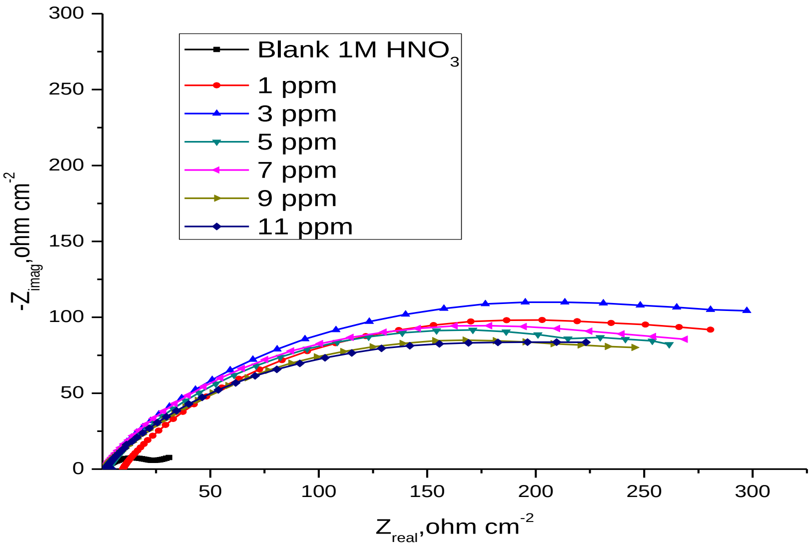

Figure 8a. The Nyquist diagrams of Cu in 1 M HNO_3 with and without various concentrations of CE at 25^OC

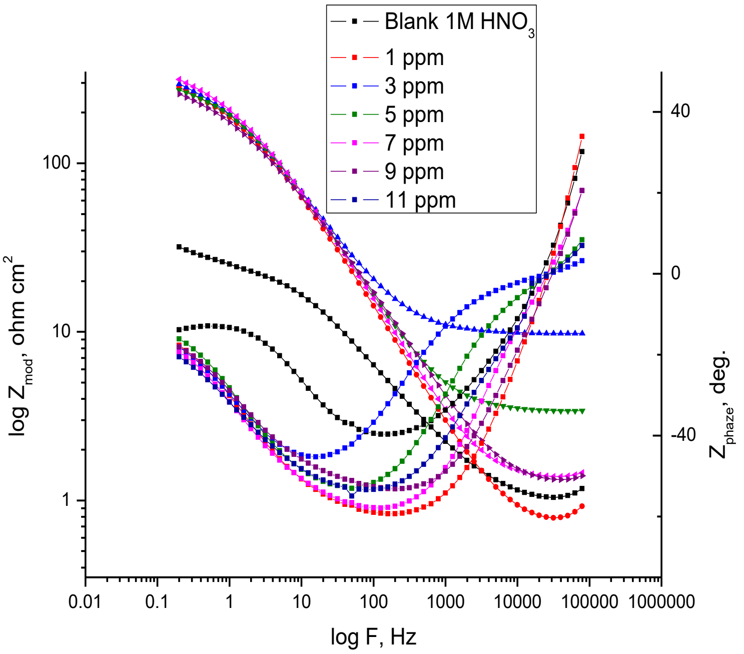

Figure 8b. The Bode diagrams for the corrosion of Cu in 1 M HNO_3 with and without various concentrations of CE at 25^OC

Table 8. EIS parameters for Cu corrosion without and with various concentrations of CE at 25°C

Concentration, ppm		R_P, Ω cm^2	C_{dl}x10^{-4}, µFcm^{-2}	Ɵ	% PE
	1M HNO_3	28.60	6.2	-----	-----
Chenopodium extract	1	272.1	4.3	0.895	89.5
	3	279.1	4.1	0.898	89.8
	5	287.5	3.7	0.901	90.1
	7	297.4	3.5	0.904	90.4
	9	336.5	3.3	0.915	91.5
	11	338.8	2.8	0.916	91.6

3.7 Electrochemical Frequency Modulation (EFM) Tests

EFM is characterized by speed and greatly accuracy in calculating the current data [46, 47]. Figure 9 indicates the EFM of Cu in 1M HNO_3 solution and various dose of CE. The EFM parameters such as (CF-2 and CF-3), (β_c and β_a) and (i_{corr}) can be measured from the higher current peaks. The CF is closer to the standard data proved the validity of the calculated data. The PE% increase with the raising of CE concentrations. The % PE_{EFM} rise by raising the CE concentrations and was measured as from Eq. (11):

$$\%PE_{EFM} = [1-(i_{corr}/i^o_{corr})] \times 100 \qquad (11)$$

Where i^o_{corr} and i_{corr} are corrosion currents with and without various concentrations of CE

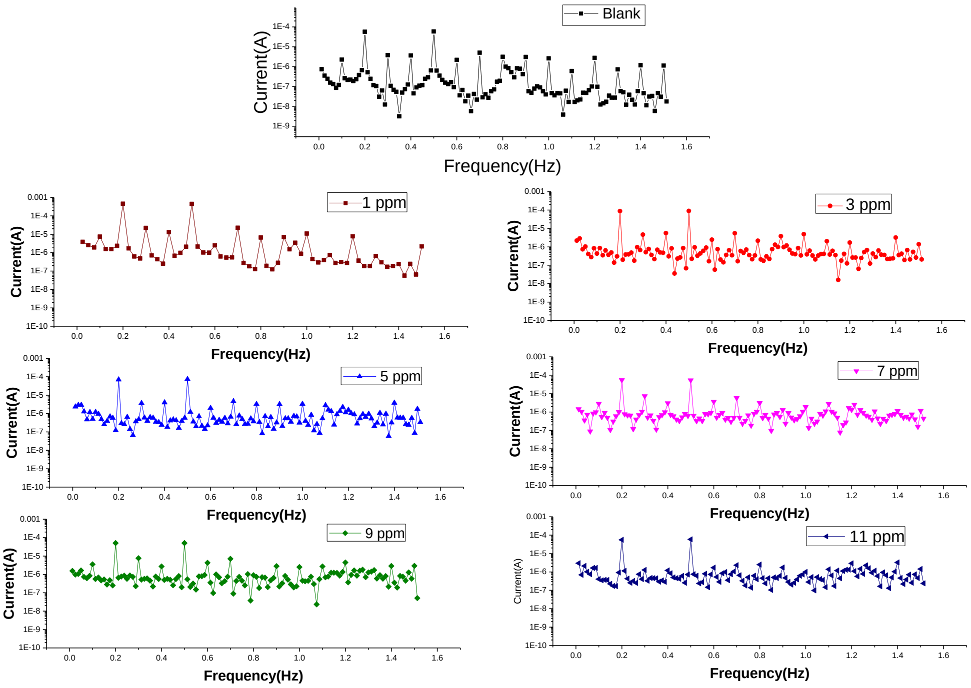

Figure 9. EFM curves for Cu dissolution without and with various concentrations of CE at 25°C

Table 9. Parameters of EFM diagrams for Cu corrosion without and with various concentrations of CE in 1 M HNO_3 at 25°C

Conc., ppm	i_{corr} μA cm^{-2}	β_a mV dec^{-1}	β_c mV dec^{-1}	CF-2	CF-3	k_{corr} mpy	% PE
Blank	523.7	63.93	91.80	2.3	3.1	258.5	-----
1	360.8	60.29	277.9	1.9	3.0	178.1	31.1
3	215.7	60.05	110.9	2.0	3.0	106.4	58.8
5	208.4	58.12	295.2	1.9	3.2	102.8	60.2
7	107.7	40.21	64.48	2.0	3.0	53.15	79.4
9	89.95	63.77	169.8	1.8	3.1	44.39	82.8
11	63.02	45.48	97.15	1.9	2.9	28.80	88.0

3.8 Scanning Electron Microscopy (SEM) Examinations

The micrographs of polished Cu surface immersed in 1 M HNO_3 solution with and without various CE (11 ppm) for 48 h at 25°C are displayed in Figure (10). It is clear that Cu surface is very smooth, while the unprotected surface which affected by corrosive medium and suffer from cracking, in the presence of the extract we found that Cu surface resist the corrosion effect it is can be qualified to the formation of film [48].

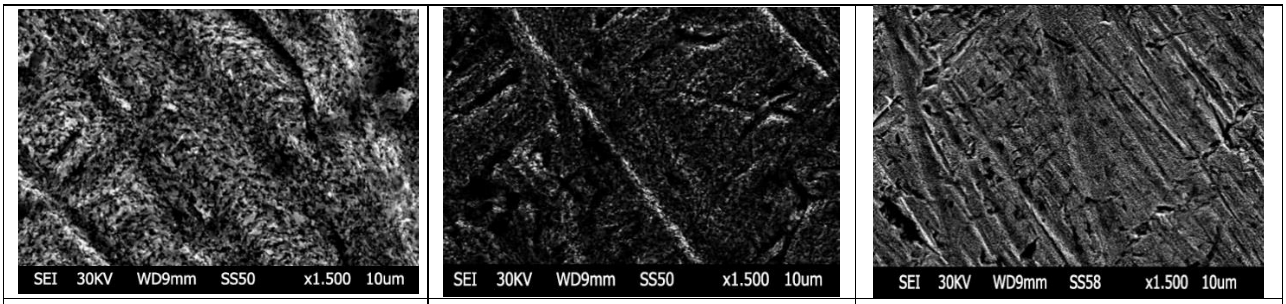

(a) **Free sample**	**(b)** **Blank**	**(c)** **1M HNO$_3$ + Chenopodium**

Figure 10. SEM micrographs of Cu surface (a) before of dipping in 1 M HNO$_3$, (b) after 48 h of dipping in 1 M HNO$_3$, (c) after 48 h of dipping in 1 M HNO$_3$+ 11 ppm of Chenopodium extract at 25°C

3.9 Atomic Force Microscope (AFM) Examinations

AFM is a remarkable technique used for measuring the surface roughness with high resolution. Many details about Cu surface morphology can be obtained from AFM measurements which help explaining the corrosion process. The three dimensional AFM images were represented in Figure (11).

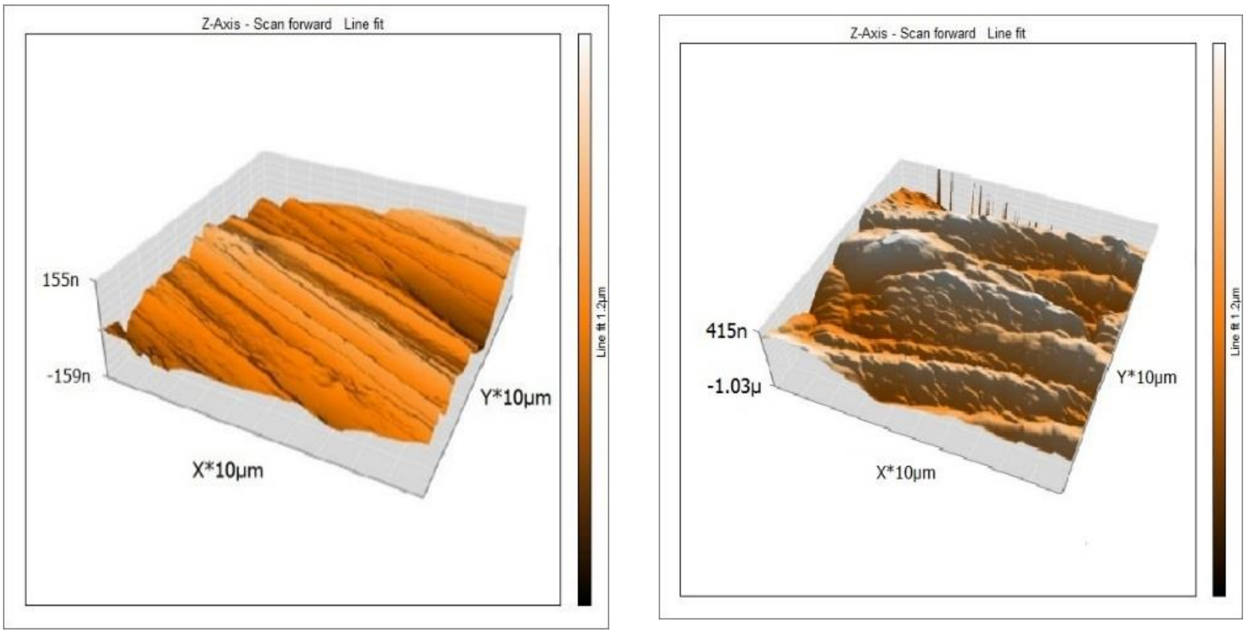

(a) Free **(b) Blank**

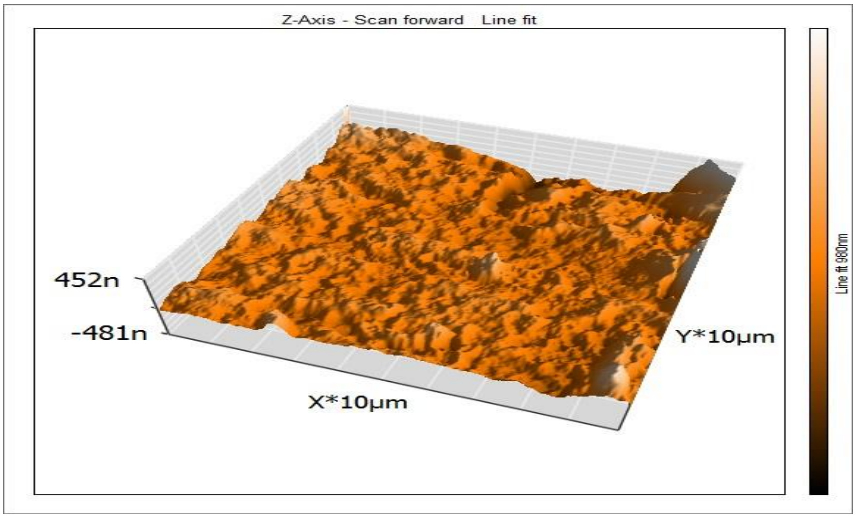

(c) Inhibitor

Figure 11. (a) 3D AFM of polished Cu, (b) 3D AFM of Cu immersed 1M HNO_3 for 1d, (c) 3D AFM image of Cu immersed in 1M HNO_3+11 ppm of extract for 1 day.

Table 10. AFM parameters of CE at 25°C

Sample	Roughness average (Sa), nm
Free	24
Blank	163
Chenopodium	52

The roughness calculated from AFM image is summarized in Table (10). The values showed that the roughness rises with adding HNO_3 due to the corrosion occurs on the Cu surface but decreased with adding the extract [49].

3.10 FTIR spectra of metal with CE

Spectra of the stock CE and Cu surface previously and after inundation in 1M HNO_3 + 11 ppm of the CE for 3 hours at 25° C is presented in Figure (12). It is obviously clear that there are no peaks on metal surface, while the Cu sample immersed in the medium with extract shows bands ,this appeared bands are similar to the stoke CE bands with small shift we found that The peaks corresponding to O-H stretch at 3357 cm^{-1} shift to 3355cm^{-1} ,and the peaks attributed to C-H stretch at 2918 cm^{-1} shift to 2921 cm^{-1} ,and the peaks of C=C stretch at 1625 cm^{-1}showd shift at 1636 cm^{-1} ,and the peaks shifted from 1730 cm^{-1} to1715 cm^{-1} can be attributed to carboxylic acid or aromatic ketones. This means that CE is completely adsorbed on Cu surface and the shifted peaks can be assigned to the interaction of adsorbed molecules of inhibitor on Cu surface. All These results complement the results of electrochemical techniques and confirm that the Chenopodium extract inhibited Cu corrosion through inhibitor adsorbed of on surface of Cu.

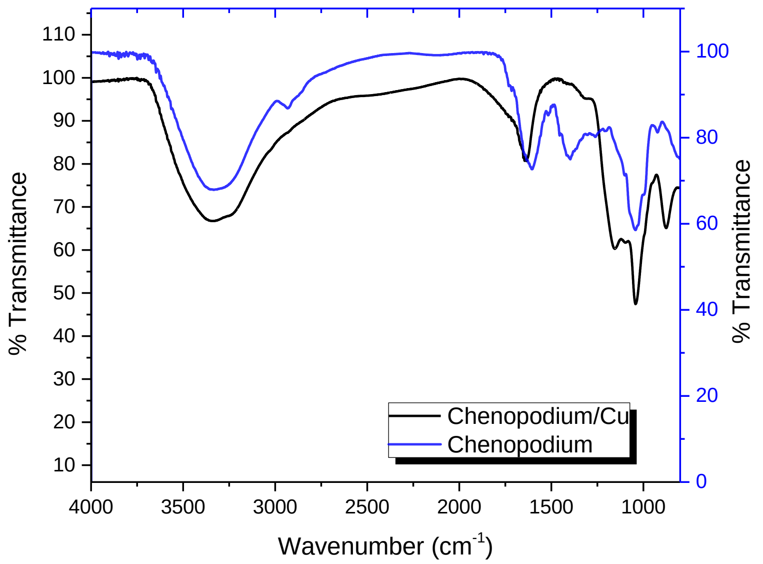

Figure 12. (a) FTIR spectra for free CE, and (b) FTIR spectra of metal with CE

4. CONCLUSIONS

CE is a best save inhibitor for corrosion of Cu in 1 M HNO_3. From all experiments, the PE increases with raising CE concentrations and lowered with elevation of temperature. Adsorption of Chenopodium on Cu surface obey Langmuir isotherm. From thermodynamic value addition of CE increases activation energy. The negative data of (ΔG^{o}_{ads}) and ΔH°_{ads} designate that adsorption has spontaneous and exothermic. PP technique suggests that CE can used as mixed type inhibitor

References

1. P. B. Raja, M. G. Sethuraman, *Materials Letters*, 62(2008)113.
2. O. K. Abiola, A. O. James, *Corrosion Science*, 52 (2010) 661.
3. P. B. Raja, M. G. Sethuraman, *Materials and Corrosion*, 60 (2009)22.
4. I. B. Obot, N. O. Obi Egbedi, *Journal of Applied Electrochemistry*, 40 (2010) 1977.
5. V. K. Singh, M. M. Singh, N. Chaubey, P. Mourya, *IJIRSET,* 4(6)(2015)4545.
6. A. S. Fouda, K. Shalabi, A. A. Idress, *Green chemistry letters and reviews,* 8(2015)17
7. A.S. Fouda, S.M. Rashwan, M.M.K. Darwish and N.M. Arman, *Portugaliae Electrochimica Acta,* 36(5) (2018) 309
8. A.S. Fouda, H.M. El-Abbasy and A.A. El-Sherbini, *Int. J. Corros. Scale Inhib.*, 7(2) (2018) 213
9. A. S. Fouda, Hisham H. Al-Zehry, M. Elsayed, J. BioTribo Corros., 4-23(2018)1
10. A.S.Fouda, H. A. Mostafa, A.F.S.Molouk, H.M. El-Saeed, *Desalination &water treatment,* 8(3) (2018)377.
11. A. S. Fouda, and E. Abdel Haleemb, *Surface Engineering and Applied Electrochemistry*, 54(5) (2018)498
12. R.Rahma, A.S. Fouda, Emad E. El-Katori, and H.A.Mostafa, *Journal of Chemical, Biological and Physical Sciences*, 8 (3) (2018) 407-428.
13. A.S.Fouda, Shady M. El – Dafrawy, Ali M. El-Azaly and Eslam S. El-hussieny, *Journal of Chemical, Biological and Physical Sciences*, 8(3)(2018) 325.
14. A.S.Fouda, R.M. Abou Shahba, A.E.El-Shenawy, T.J.A. Seyam, *Int. J. Electrochem. Sci.*, 13 (2018) 7057

15. A.S.Fouda, R.M.Abou Shahba, A.E.El-Shenawy and T.J.A.Seyam, *Chemical Science Transactions,* 7(2) (2018) 163
16. A. S. Fouda, K. Shalabi, A. M. Nofal and M. A. El-Zekred, *Chemical Science Transactions,* 7(1) (2018) 101
17. A. B.Gadano, A. A.Gurni, M. A.Carballo, *Journal of Ethnopharmacology, Copenhagen,*103(2) (2006) 246.
18. G. F.Vita, I.Ferreira, M. A. V. C. da Pereira, A.Sanavria, R. C. M.Aurnheimer, C. G. Barbosa, S. S. M. E.Gallo, H. V. G.Vasconcellos, *Pesquisa Veterinária Brasileira*, Seropédica, 35 (5) (2015) 424.
19. G. D. Silva, *Dissertação (Ciência Animal nos Trópicos)* –Universidade Federal da Bahia, Bahia.
20. M.Reis, A.Trinca, M. J.Ferreira, A. R.Monsalve, M. A. Grácio, *Experimental Parasitology,* Berlin, 126(2) (2010) 191.
21. G. N.Mu, T. P. Zhao, M. Liu, T. Gu, *Corrosion*, 52(1996)853.
22. K. F. Khaled, *Mater. Chem. Phys*., 112(2008)290.
23. R. W. Bosch, J. Hubrecht, W. F. Bogaerts, B. C. Syrett, *Corrosion*, 57(2001)60.
24. S. S. Abdel–Rehim, K. F. Khaled, N. S. Abd–Elshafi, *Electrochim. Acta*., 51(2006)3269.
25. T. P. Hour, R. D. Holliday, *J Appl Chem*., 3(1953)502.
26. L. O. Riggs, T. J. Hurd, *Corrosion*, 23(1967)252.
27. G. M. Schmid, H. J. Huang, *Corros Sci*., 20(1980)1041.
28. A.S.Fouda, A.AEl-Hossiany, H.M.Ramadan, *Zastita Materijala*, 58(4) (2017) 541-555
29. F. Bentiss, M. Lebrini, M. Lagrenee, *Corros Sci*., 47(2005)2915.
30. A. Yurt, G. Bereket, A. Kivrak, A. Balaban, B. Erk, *J. ApplElectrochem*, 35(2005) 1025.
31. G. Banerjee, S. N. Malhotra, *Corrosion*, 48(1992)10.
32. D.C. Silverman, J. E. Carrico, *Corrosio*n, 44(1988)280.
33. W. J.Lorenz, F. Mansfeld, *Corros. Sci*., 21(1981)647.
34. F. Mansfeld, *Corrosion*, 36(1981)301.
35. M. El Achouri, S. Kertit, H. M. Gouttaya, B. Nciri, Y. Bensouda, L. Perez, M. R. Infante, K. Elkacemi, *Prog. Org. Coat*., 43(2001)267.
36. J. R. Macdonald, W. B. Johanson., in: J.R. Macdonald (Ed.), Theory in Impedance Spectroscopy, John Wiley& Sons, New York, 1987.
37. S. F. Mertens, C. Xhoffer, B. C. Decooman, E. Temmerman, *Corrosion*, 53(1997)381.
38. G. Trabanelli, C. Montecelli, V. Grassi, A. Frignani, *J. Cem. Concr., Res*., 35(2005)1804.
39. A. J. Trowsdate, B. Noble, S .J. Haris, I.S. R. Gibbins, G. E. Thomson, G. C. Wood, *Corros. Sci*., 38(1996)177.
40. F. M. Reis, H. G. De Melo, I. Costa, *Electrochim. Acta*., 51(2006)17.
41. M. Lagrenee, B. Mernari, M. Bouanis, M. Traisnel, F. Bentiss, *Corros. Sci*., 44(2002)573.
42. E. McCafferty, N. Hackerman, *J. Electrochem. Soc*., 119(1972)146.
43. H. Ma, S. Chen, L. Niu, S. Zhao, S. Li, D. Li, *J. Appl. Electrochem*., 32(2002)65.
44. E. Kus, F. Mansfeld, *Corros. Sci*., , 48(2006)965.
45. G. A. Caigman, S. K. Metcalf, E. M. Holt, *J. Chem. Cryst*., 30(2000)415.
46. C. B. Verma, M. A. Qurishi, A.J. Singh, *Taiwan Inst Chem Eng*., 49(2015)2229
47. S. B. Pralhibha, P. Kotteeswaran, V. Bheema Raju, *IOSR Journal of Applied Chemistry* (IOSRJAC) 2(2012)45.
48. D. P. Schweinsberg, A. Graeme, George, A.K. Nanayakkara, D.A. Steinert, *Corros. Sci*., 19(4) (1988)28.
49. Da-quan Zhang, Li-Xin Gao, Guo-ding Zhou, *Corros.Sci*., 46(2004) 3031-3040